# Algebraic Decay in Self-Similar Markov Chains

**James D. Hanson,** [1,2] **John R. Cary,** [1,3] **and James D. Meiss** [1]

A continuous-time Markov chain is used to model motion in the neighborhood of a critical invariant circle for a Hamiltonian map. States in the infinite chain represent successive rational approximants to the frequency of the invariant circle. For the case of a noble frequency, the chain is self-similar and the nonlinear integral equation for the first passage time distribution is solved exactly. The asymptotic distribution is a power law times a function periodic in the logarithm of the time. For parameters relevant to the critical noble circle, the decay proceeds as $t^{-4.05}$.

## 1. INTRODUCTION

A continuous-time Markov chain is defined to be self-similar if the transition probability from state $i$ to state $j$, $p_{ij}$, has the scaling property

$$p_{i+k,j+k} = \varepsilon^k p_{ij}$$

In this paper the general self-similar Markov chain with nearest-neighbor interactions (birth and death process) is considered, and the first passage time distribution is obtained exactly.

Our motivation for this study comes from the dynamics of Hamiltonians with two degrees of freedom. In such systems one would like to understand the statistics of the motion in an irregular component of phase space. Previous studies indicate that the dominant long-time effect is due to the "stickiness" [1-3] of the invariant tori which bound the irregular

---

[1] Institute for Fusion Studies, The University of Texas at Austin, Austin, Texas 78712.
[2] Present address: Department of Physics, Auburn University, Auburn, Alabama 36849.
[3] Present address: Department of Astrophysical, Planetary, and Atmospheric Sciences, University of Colorado, Boulder, Colorado 80309.

region, e.g., the outermost torus enclosing a regular island. These boundary tori are "critical": any perturbation will destroy them.[4] Motion in the irregular region in the neighborhood of a critical torus is governed by an infinite sequence of slightly broken tori, called cantori, through which orbits must weave.[5] A description of the flux of orbits through cantori leads to a Markov chain model for the stochastic dynamics. The case of a critical torus with "noble" frequency has been studied using renormalization methods.[4] These show that the properties of the cantori have scaling properties which lead to the self-similar scaling of the transition probabilities.

The purpose of developing such a model is to enable one to calculate the statistics of trapping near the critical torus. Of particular interest is the first passage time distribution, $R_{10}(t)$, the probability per unit time of the first arrival in state zero for a particle in state one at $t = 0$. This represents the probability distribution of the first exit from the region near the boundary. The asymptotic behavior of $R_{10}$ depends on those orbits arbitrarily close to the boundary, and is thus expected to have a universal form. As has been discussed by Karney,[1] the correlation function and the "diffusion" coefficient can be obtained from $R$.

The solution of the self-similar Markov chain proceeds by considering the first passage distributions $R_{10}(t)$ and $R_{21}(t)$. Standard probability theory gives one relation between these two quantities. A second relation is obtained from self-similarity. These two relations combine to give a nonlinear integral equation for $R_{10}(t)$. The Laplace transform of this equation yields a nonlinear algebraic equation involving the transform $\hat{f}(s)$ at two different values of the Laplace variable $s$. Use of a particular ansatz reduces the problem to a finite difference equation in $\ln(s)$.

The finite difference equation is nonstandard because the independent variable has a continuous rather than discrete domain. As a result there are an infinite number of solutions, which can be related to two basic functions by linear composition with functions periodic in $\ln(s)$. To understand the solution space and to answer questions of existence and uniqueness, methods similar to those of the theory of linear differential equations are developed and used. Finally, the unique physical solution is obtained by imposing boundary conditions.

The final expression for the Laplace transform is expressed in terms of infinite sums of elementary functions. A single constant must be determined numerically or by perturbation methods. The asymptotic ($t \to \infty$) behavior of the return distribution $R_{10}(t)$ is determined by the behavior of the transform $\hat{f}(s)$ near the origin ($s \to 0$), where $\hat{f}(s)$ has a branch point. Standard techniques allow one to deduce that $R_{10}(t)$ has the asymptotic form $R_{10}(t) \sim h(t)t^{-\alpha}$, where $h(t)$ is periodic in $\log(t)$. The decay power $\alpha$ and the

function $h(t)$ are determined by the parameters describing the Markov chain. For parameters relevant to the Hamiltonian model, $\alpha = 4.05$.

The outline of the paper follows. In Section 2 the development of the self-similar Markov chain as a model for motion near a regular region is discussed. Section 3 contains the analysis of the self-similar Markov chain. In Section 4, the results of this model are compared with previous numerical studies of the statistics.

## 2. MARKOV MODEL OF FLUX THROUGH CANTORI

Two-degree-of-freedom Hamiltonian flow can be reduced to an area-preserving map by the surface-of-section method. Invariants of the system restrict the motion to tori in phase space or equivalently to topological circles on the surface-of-section. On each circle, motion is conjugate to a rotation with some frequency, $\omega$. For the integrable system, the entire surface is filled with such circles. Upon perturbation (represented by the amplitude $k$) some of the circles are destroyed; those with frequencies close to low-order rationals disappear first. The value of the perturbation parameter leading to destruction of a circle of frequency $\omega$, $k_{cr}(\omega)$, is a fractal function of the frequency.[6] The destruction of an invariant circle is analogous to a phase transition, and can be treated using a version of the renormalization group.[4,7] At the critical point of the renormalization group, $k_{cr}$, the neighborhood of the invariant circle has a self-similar structure.

This structure can be best understood in terms of the continued fraction expansion for the frequency:

$$\omega = [l_0, l_1, l_2,...] = l_0 + 1/(l_1 + 1/(l_2 + \cdots \tag{1}$$

The renormalization structure is obtained by successive truncations of this continued fraction. The $m$th convergent is a rational frequency, $\omega_m$. Typically, this rational frequency determines two periodic orbits, one hyperbolic and one elliptic (at $k_{cr}$), corresponding to a chain of islands in the phase space. Stochastic orbits in the neighborhood of the critical circle meander through the "levels" corresponding to the various convergents, becoming trapped near chains of islands. Three such chains are shown in Fig. 1.

The relationship between the motion at one level and that at the next is obtained through the renormalization transformation. We will use only a few simple properties of the renormalization; more details are available in Ref. 7. The renormalization transformation maps one island at level $m$ onto one at level $m + 1$. The coordinate transformation includes an area rescal-
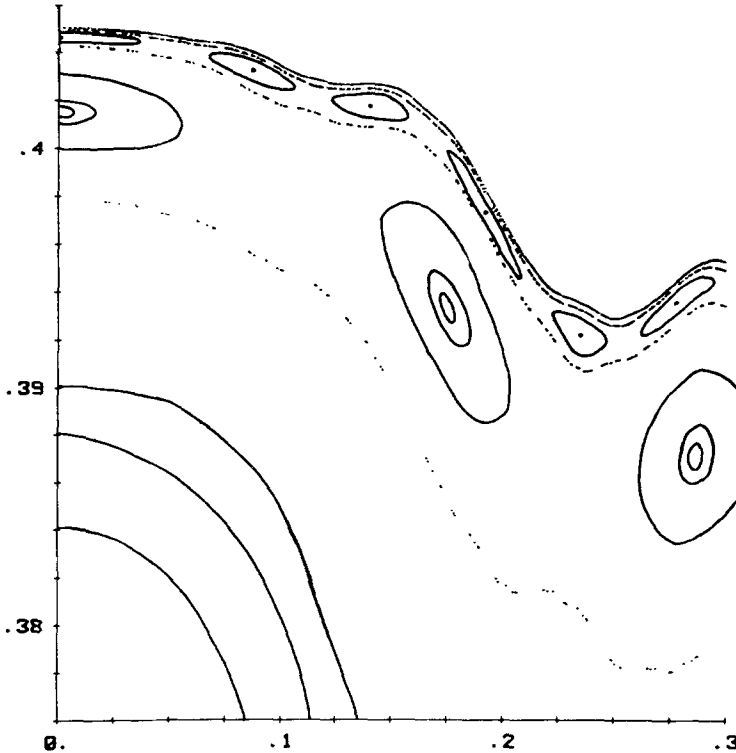
Fig. 1. Phase Space of the standard map in symmetry coordinates[4,5] at $k_{cr}$ for $\omega = 1/g^2$. Shown is a portion of one island with $\omega = 3/8$, three islands with $\omega = 8/21$, and six islands with $\omega = 21/55$, corresponding to levels 4, 6, and 8. The uppermost curve is the critical noble circle and below it are the three cantori with minimum $\Delta W$ between each pair of island chains. The states in the Markov chain are the stochastic regions bounded by a pair of cantori and excluding the island chains.

ing to accomplish this map. Since successive convergents bracket $\omega$ (the odd being larger and the even smaller than $\omega$), and we treat stochastic motion trapped on one side of the critical circle, we consider the even iterates of the transformation. Its form depends in detail on the particular frequency considered; the simplest case is that of "noble" frequencies.

A noble irrational is defined as having a continued fraction such that $l_m = 1$ for all $m > m_0$ for some $m_0$. Nobles are the most difficult to approximate by rationals, and thus are expected to withstand perturbation best. This is born out by numerical calculation. One expects that in any region of phase space the most noble circles will tend to be the last

destroyed (which is not say that the outermost invariant circle of an island is typically noble). The "king" of nobles is the golden mean,

$$g = [1, 1,...] = (1 + \sqrt{5})/2 \tag{2}$$

which we exclusively consider below. However, the region near enough to any noble is dominated by its golden tail. This is significant since, as shown below, the long-time properties of the system are governed by the orbits trapped very close to the critical circle. We will only need two simple properties of the rescaling transformation for the golden critical circle: the ratio of the area of an island of the $m$th convergent to that of the $(m + 2)$th is [4,7]

$$\xi^2 \cong 18.828692 \tag{3}$$

and the period, $q_m$, of the $m$th convergent scales as

$$q_m \cong g^m \tag{4}$$

In Fig. 1 three levels of this scaling are shown.

　　　To construct a model for stochastic motion in the neighborhood of a critical noble circle, it is necessary to understand the mechanism for transitions from one level to the next.[5] The important barriers are the remnants of destroyed invariant circles called cantori.[8] A cantorus is an invariant Cantor set with a definite rotation frequency. The gaps in the cantorus can be though of as being formed by nearby island chains attempting to overlap. While an invariant circle is an absolute barrier to motion, orbits can leak though the gaps in a cantorus. The rate at which they do so is determined by the flux through the cantorus, $\Delta W$, defined as the area which crosses the cantorus in one iteration of the map. By area preservation the same amount of area returns on each iteration. It can be shown that the flux can be calculated as a difference in action between the cantorus and an orbit homoclinic to it, $\Delta W = W_h - W_c$, which is the reason for the notation.[5]

　　　There is a cantorus for every destroyed invariant circle with irrational frequency. Most of these cantori should be relatively unimportant in the determination of the transport of stochastic orbits through phase space. Those cantori with locally minimum values of $\Delta W$ will be the limiting barriers. To the extent that the function $\Delta W(\omega)$ has only a few sharp minima, it may be possible to neglect all but a few of the cantori. The quantity $\Delta W$ is in fact a fractal function of frequency similar in form to $k_{cr}$; it appears to have a local minimum at every noble frequency (a countably infinite set). In the neighborhood of a critical noble circle there are noble cantori between the convergent island chains. These cantori also scale

according to the renormalization transformation (see Fig. 1). The cantori with the minimum $\Delta W$ between levels will be referred to as "minimizing."

To develop the model we introduce our primary approximation of treating the motion of an orbit trapped at the $m$th level as random. Numerical computations show that the transitions from level to level occur suddenly, and that the time an orbit is trapped at one level is large compared to the iteration period of the map. A particle at level $m = 2j$ will be referred to as in state $j$. We assume that successive transitions are uncorrelated and can therefore be described by transition probabilities, $p_{ij}$, from state $i$ to state $j$. These probabilities are determined by the ratio of the flux, $\Delta W_{ij}$, through the minimizing cantorus connecting states $i$ and $j$ to the area accessible to the particle in state $i$, $A_i$:

$$p_{ij} = \Delta W_{ij}/A_i \tag{5}$$

Since we assume $p_{ij}$ is independent of the detailed history of the motion the dynamics can be described by a Markov chain. When the transition probabilities are small the Markov chain can be taken to have continuous time:

$$\frac{dN_j}{dt} = \sum_i N_i p_{ij} \tag{6}$$

where $N_j$ is the mean number of particles in state $j$.

The scaling of the transition probabilities with level is easily computed from Eqs. (3)–(5). The flux scales as the area coefficient

$$\Delta W_{j,j+1} = \Delta W_{j+1,j} = \Delta W_{01}/\xi^{2j} \tag{7}$$

By contrast the area of state $j$ scales as the period of the orbit (the number of islands) times the fundamental area (the area of a single island):

$$A_j = A_0(g/\xi)^{2j} \tag{8}$$

This shows that the transition probabilities scale as

$$p_{j,j+1} = p_{01}\varepsilon^j \tag{9}$$

with the factor $\varepsilon = g^{-2}$. The probability of a transition from $j$ to $j+1$ differs from the probability of the reverse transformation by the factor

$$p_{j,j+1}/p_{j+1,j} = \mu = (g/\xi)^2 \tag{10}$$

which is related to the scaling of $A_j$.

Decreasing $j$ corresponds to moving away from the critical circle. Far from the critical circle the scaling property no longer holds, but the motion is strongly stochastic. The time an orbit is trapped in the self-similar region can be obtained from the first passage time distribution $R_{10}(t)$. Here we think of state zero as representing that part of phase space far from the critical circle. The first passage time distribution is calculated in Section 3.

The Markov chain model has several obvious defects for describing the dynamics near a noble critical circle. The first is that only a countable number of the uncountable infinity of cantori have been included. While there is numerical evidence that the cantori with large $\Delta W$ between minimizing cantori can be ignored, this has not been verified in detail. A more serious defect of the model is that arbitrarily close to any minimizing cantorus is another with nearly the same value of the flux (it is known that $\Delta W$ is a continuous function on the irrationals[9]). These cantori cannot be straightforwardly included in the model, since the Markovian approximation is invalidated when the area between the cantori becomes of order $\Delta W$. However, it is possible that the structure consisting of the minimizing cantorus and its neighbors can be treated as one barrier with some effective flux. In this case the scaling properties for this flux will still be given by Eq. (7) and the model will still hold.

Another defect is that, as well as the "main branch" of cantori included above, there is also an infinite sequence of cantori surrounding each island. These cantori, which are formed from destroyed invariant curves inside the island "separatrix," could easily be formally included in the model. In this case the topology of the Markov chain is that of a "tree." The branching probabilities for this tree are given in terms of the $\Delta W$ of the island cantori.

Finally we note that it is unlikely that the rotation number of the typical boundary circle is noble.[10] Unlike the "last" invariant circle in a region of phase space, which is isolated, the typical boundary circle, such as the outermost circle about an island, is expected to have KAM surfaces on one side. This implies that its frequency is not noble; therefore, the strict self-similarity of Eq. (9) does not apply. However, it is likely that a statistical self-similarity applies, with $\varepsilon$ being given probabilistically.

While the self-similar Markov chain model is motivated by the description of transport near a critical noble circle, our treatment, presented in the next section, is valid for a general nearest-neighbor, self-similar Markov chain.

## 3. FIRST PASSAGE DISTRIBUTION FOR THE SELF-SIMILAR, NEAREST-NEIGHBOR MARKOV CHAIN

### 3.1. Model and Definition of First Passage Time Distributions

The transition probability matrix of a general Markov chain with only nearest-neighbor interactions has the form

$$p_{ij} = a_i \delta_{i-1,j} + b_i \delta_{ij} + c_i \delta_{i+1,j} \tag{11}$$

The self-similarity property (9) implies $a_i = a\varepsilon^i$, $b_i = b\varepsilon^i$, and $c_i = c\varepsilon^i$. Time can be scaled to set $b_1 = -1$. The ratio $c/a \equiv \mu\varepsilon$ is defined in according with Eq. (10). Imposition of particle conservation,

$$\sum_j p_{ij} = 0$$

completes the spcification of the coefficients, $a = 1/\varepsilon(1 + \mu\varepsilon)$, $b = -1/\varepsilon$, and $c = \mu(1 + \mu\varepsilon)$. The resulting equation for the probability evolution,

$$\frac{dN_j}{dt} = \varepsilon^{j-1} \left[ \frac{\mu}{1 + \mu\varepsilon} N_{j-1} - N_j + \frac{\varepsilon}{1 + \mu\varepsilon} N_{j+1} \right] \tag{12}$$

has the scaling properties discussed in Section 2. As can be seen in this equation, self-similarity implies that time is effectively rescaled by $\varepsilon$ when $j$ is increased by unity.

The solution proceeds by considering first passage time distributions. The first passage time distribution $R_{ij}(t)$ is the probability that a particle in state $i$ at time zero first reaches state $j$ at time $t$. The direct first passage time distribution, $R_{ij}^d(t)$, is the probability that a particle in state $i$ at time zero first reaches state $j$ at time $t$ without having been in another state between times zero and $t$. The distribution $R_{ij}^d(t)$ vanishes whenever $p_{ij} = 0$, since then state $j$ is not directly accessible from state $i$, and in general is given by

$$R_{ij}^d(t) = p_{ij} \exp(p_{ii}t) \tag{13}$$

Our goal is to calculate $R_{10}(t)$. The physical interpretation arises from thinking of the states $n = 1,..., \infty$ as being deep in the cantori sequence, so that a particle enters the chain by first being in state one. The particle leaves the chain when it arrives at state zero. Thus, $R_{10}$ gives the statistics of leaving the chain given that the particle entered the chain at $t = 0$.

For the general self-similar Markov chain, $\mu$ and $\varepsilon$ are positive, but otherwise arbitrary. In our analysis we assume that $\varepsilon$ is less than unity, in

correspondence with the cantori model. The analysis can be readily modified for $\varepsilon \geqslant 1$.

## 3.2. Integral Equation for $R_{10}(t)$

The passage distribution $R_{10}(t)$ obeys

$$R_{10}(t) = R_{10}^d(t) + \int_0^t dt_1 \, R_{12}^d(t_1) \, R_{20}(t - t_1) \tag{14}$$

This equation is obtained by noting that particles arriving in state zero from state one are of two classes. The first class, represented by $R_{10}^d$, consists of those that make a transition directly from state one to state zero. The second class consists of those that make a transition directly from state one to state two before arriving at zero. Their contribution to $R_{10}(t)$ comes from the integral over $t_1$ (the time at which the first transition out of state one is made).

In Eq. (14), both $R_{10}^d$ and $R_{12}^d$ are known from Eq. (13), while $R_{20}$ is as yet unknown. For a nearest-neighbor chain, one can write

$$R_{20}(t) = \int_0^t dt_1 \, R_{21}(t_1) \, R_{10}(t - t_1) \tag{15}$$

since in order for a particle to get from state two to state zero, it must have first entered state one at some time $t_1$. Substituting Eq. (15) into Eq. (14), one obtains

$$R_{10}(t) = R_{10}^d(t) + \int_0^t dt_1 \, R_{12}^d(t_1) \int_{t_1}^t dt_2 \, R_{21}(t_2 - t_1) \, R_{10}(t - t_2) \tag{16}$$

For a self-similar chain, because of the time rescaling, Eqs. (11) and (13) imply

$$R_{i+1,i}^d(t) = \varepsilon R_{i,i-1}^d(\varepsilon t) \tag{17}$$

This rescaling property is valid for the full first passage time distribution as well:

$$R_{i+1,i}(t) = \varepsilon R_{i,i-1}(\varepsilon t) \tag{18}$$

Together, Eqs. (16) and (18) yield

$$R_{10}(t) = R_{10}^d(t) + \varepsilon \int_0^t dt_1 \, R_{12}^d(t_1) \int_{t_1}^t dt_2 \, R_{10}(\varepsilon t_2 - \varepsilon t_1) \, R_{10}(t - t_2) \tag{19}$$

the nonlinear equation to be solved.

## 3.3. Reduction to a Linear Difference Equation

Equations (13) and (19) imply

$$f(t) = e^{-t} + v\varepsilon \int_0^t dt_1 \, e^{-t_1} \int_{t_1}^t dt_2 \, f(\varepsilon t_2 - \varepsilon t_1) \, f(t - t_2) \qquad (20)$$

in which $v \equiv \mu\varepsilon(1 + \mu\varepsilon)^{-2}$; and the new dependent variable is $f(t) \equiv (1 + \mu\varepsilon) R_{10}(t)$. From Eq. (20) one can deduce that the Laplace transform,

$$\hat{f}(s) \equiv \int_0^\infty e^{-st} f(t) \, dt \qquad (21)$$

must satisfy an algebraic equation,

$$\hat{f}(s) = [1 + s - v\hat{f}(s/\varepsilon)]^{-1} \qquad (22)$$

that relates the values of $\hat{f}$ at different values of the dependent variable.

Equation (22) can be used to determine the large-$s$ asymptotic form of $\hat{f}(s)$. There are actually two possibilities. From Eq. (21) one can see that the physical solution asymptotes to zero. Therefore, Eq. (22) implies

$$\hat{f}(s) \sim (1 + s)^{-1} \qquad (23)$$

One can also see from Eq. (22) the second possible asymptotic behavior,

$$\hat{f}(s) \sim (\varepsilon s + 1)/v \qquad (24)$$

One can convert the nonlinear equation (22) to a linear difference equation by use of the ansatz,

$$\hat{f}(s) = Q(s/\varepsilon)/Q(s) \qquad (25)$$

For the physical solution, which from Eq. (21) must be everywhere positive, this ansatz is valid, as can be seen by constructing $Q(s)$ as follows. On any interval $s_0 \leqslant s < s_0/\varepsilon$, $Q(s)$ is chosen to be some nonzero (but otherwise arbitrary) function. For $s \geqslant s_0/\varepsilon$, $Q$ is defined recursively by $Q(s) = Q(s\varepsilon) \hat{f}(s\varepsilon)$, while for $s < s_0$, $Q$ is defined recursively by $Q(s) = Q(s/\varepsilon)/\hat{f}(s)$. It is not hard to show that $Q(s)$ can be chosen to have an arbitrary number of derivatives. With this ansatz one obtains the linear equation,

$$Q(s) = (1 + s) \, Q(s/\varepsilon) - vQ(s/\varepsilon^2) \qquad (26)$$

involving the value of $Q$ at three different argument values. In terms of the variable $\ln(s)$, Eq. (26) is a linear difference equation. In fact, any nonlinear

equation of the form, $A(s) \hat{f}(s) \hat{f}(s/\varepsilon) + B(s) \hat{f}(s) + C(s) = 0$, is transformed into the linear equation, $A(s) Q(s/\varepsilon^2) + B(s) Q(s/\varepsilon) + C(s) Q(s) = 0$, by the ansatz (25).

## 3.4. Solution Space of the Linear Difference Equation

**3.4.1. General Theory.** It is easy to show that if $Q(s)$ is a solution to Eq. (26), then $Q(s) q(s)$ is also a solution to Eq. (26), provided $q(s)$ is *log periodic*, $q(s/\varepsilon) = q(s)$. One can also see that any two solutions that are equal on an interval $s_0 \leqslant s < s_0'/\varepsilon^2$ must be equal everywhere. To precisely determine the extent of the solution space one must analyze this equation along the lines of the theory of linear differential equations.

Consider the generalized Wronskian,

$$W(Q_1, Q_2, s) \equiv Q_1(s) Q_2(s/\varepsilon) - Q_1(s/\varepsilon) Q_2(s) \qquad (27)$$

of any two functions $Q_1$ and $Q_2$. If $Q_1$ and $Q_2$ are solutions to Eq. (26), then

$$W(Q_1, Q_2, s/\varepsilon) = W(Q_1, Q_2, s)/\nu \qquad (28)$$

Thus, $W$ is nonzero everywhere provided it is nonzero on any interval $s_0 \leqslant s < s_0/\varepsilon$.

With this knowledge we can prove that given any two solutions $Q_1(s)$ and $Q_2(s)$ of Eq. (26) with nonvanishing Wronskian, any third solution $Q(s)$ can be put in the form

$$Q(s) = q_1(s) Q_1(s) + q_2(s) Q_2(s) \qquad (29)$$

where $q_1$ and $q_2$ are log periodic. To see this, one defines $q_1$ and $q_2$ on an interval $s_0 \leqslant s < s_0/\varepsilon$ by the equations

$$Q(s) = q_1(s) Q_1(s) + q_2(s) Q_2(s)$$

and

$$Q(s/\varepsilon) = q_1(s) Q_1(s/\varepsilon) + q_2(s) Q_2(s/\varepsilon)$$

The solutions for $q_1$ and $q_2$ are well defined since $W \neq 0$. Outside the interval $s_0 \leqslant s < s_0/\varepsilon$ the functions $q_1$ and $q_2$ are defined by log periodicity. With this construction Eq. (29) is valid since both sides of the equation are solutions to Eq. (26) and the two solutions agree over an interval $s_0 \leqslant s < s_0/\varepsilon^2$.

### 3.4.2. Small-$s$ Solutions.

To explicitly construct two solutions of Eq. (26) one can use Frobenius series,

$$Q(s) = s^\gamma \sum_{n=0}^{\infty} a_n s^n \tag{30}$$

Insertion of the form (30) into Eq. (26) and matching coefficients yields the equation,

$$\varepsilon^{2\gamma} - \varepsilon^\gamma + \nu = 0 \tag{31}$$

for the exponent. The two solutions,

$$\gamma_\pm \equiv \ln[\tfrac{1}{2} \pm \tfrac{1}{2}(1 - 4\nu)^{1/2}]/\ln(\varepsilon) \tag{32}$$

are real (since $\nu \leqslant 1/4$) and satisfy $0 < \gamma_+ \leqslant \gamma_-$. Particular solutions $Q_+$ and $Q_-$ are obtained by choosing $a_0 = 1$ and the higher coefficients by the recursion relation

$$a_n^\pm = a_{n-1}^\pm \, \varepsilon^{n + \gamma_\pm + 1}/(\nu - \varepsilon^{n + \gamma_\pm} + \varepsilon^{2n + 2\gamma_\pm}) \tag{33}$$

As can be seen from Eq. (33), the radius of convergence is infinite since $\lim_{n \to \infty} a_n/a_{n-1} = 0$.

A special case occurs if the two exponents differ by an integer, $\gamma_- = \gamma_+ + l$. Then the solution $Q_+(s)$ is not valid because the denominator in the recursion relation (33) vanishes for $n = l$. To find the second solution one must use theory similar to that of an ordinary linear differential equation with a regular singular point whose indicial roots differ by an integer. We do not discuss this special case further here.

In the limit $s \to 0$, the Wronskian of these two solutions is

$$W(Q_+, Q_-, s) = (1 - 4\nu)^{1/2}(s/\varepsilon)^{\gamma_+ + \gamma_-}[1 + O(s)]$$

Since $W \neq 0$ for an interval $s_0 \leqslant s < s_0/\varepsilon$ when $s_0$ is small, $W$ nowhere vanishes. Therefore, any solution, and in particular the physical solution, can be written

$$Q(s) = q_+(s) \, Q_+(s) + q_-(s) \, Q_-(s)$$

### 3.4.3. Large-$s$ Solutions.

The large-$s$ behavior of $Q(s)$ can be analyzed with an expansion,

$$Q(s) = s^{k \ln s + h} \sum_{n=0}^{\infty} b_n s^{-n} \tag{34}$$

around $s = \infty$. Substitution of this form into Eq. (26) and matching coefficients yields two solutions.

The first solutions, $Q_g(s)$, grows as $s \to \infty$. It has $k = k_g \equiv -1/2 \ln \varepsilon$, which is positive, and $h = h_g \equiv -3/2 + \ln \nu / \ln \varepsilon$. The recursion relation for the coefficients,

$$b_n^g = (b_{n-1}^g / \varepsilon - \nu b_{n-2}^g / \varepsilon^{n+1}) / (\varepsilon^n - 1) \qquad \text{for} \quad n \geqslant 2 \tag{35}$$

implies a large $n$ behavior of $b_n^g \sim \varepsilon^{-(n - n_g)^2/4}$. Thus, this series has a radius of convergence of zero and, so, is only asymptotic. To specify a unique series, the choice $b_0^g = 1$ is made.

The second solution, $Q_d(s)$, decays as $s \to \infty$. It has $k = k_d \equiv 1/2 \ln \varepsilon$, which is negative, and $h = h_d \equiv 1/2$. The recursion relation,

$$b_n^d = (b_{n-1}^d / \varepsilon - \nu \varepsilon^{n-3} b_{n-2}^d) / (\varepsilon^{-n} - 1) \tag{36}$$

for the coefficients implies a large-$n$ behavior of $b_n^d \sim \varepsilon^{n^2/2}$. Therefore, this series has an infinite radius of convergence. Again the choice $b_0^d = 1$ is made to specify a unique series.

Two points about these solutions should be made. The first is that the Wronskian is nonzero,

$$W(Q_g, Q_d, s) \sim -\varepsilon s^{\ln \nu / \ln \varepsilon} / \nu$$

for large $s$. Therefore, $Q_g$ and $Q_d$ can be used in representations of the form (29). Second, even though the series representation of $Q_g(s)$ is valid only for large $s$, it may be extended to all $s$ by iteration of Eq. (26).

## 3.5. Imposition of the Physical Boundary Conditions

From the previous section one knows that the physical solution can be written,

$$Q_p(s) = g_p(s) Q_g(s) + d_p(s) Q_d(s)$$

in terms of the functions $Q_g$ and $Q_d$ and some yet to be determined log periodic functions $g_p$ and $d_p$. According to Eq. (25), $\hat{f}(s)$ is given by

$$\hat{f}(s) = \frac{g_p(s) Q_g(s/\varepsilon) + d_p(s) Q_d(s/\varepsilon)}{g_p(s) Q_g(s) + d_p(s) Q_d(s)}$$

If $g_p(s) \neq 0$, then the terms containing $Q_g$ in both the numerator and denominator dominate for large $s$. This gives

$$\hat{f}(s) \sim Q_g(s/\varepsilon) / Q_g(s) \sim \varepsilon s / \nu$$

the unphysical behavior found previously [Eq. (24)]. Therefore, we conclude that

$$g_p(s) = 0$$

This way, the asymptotic behavior is

$$\hat{f}(s) = Q_d(s/\varepsilon)/Q_d(s) \sim 1/s \tag{37}$$

the correct physical behavior. The function $d_p(s)$ cannot be determined. However, this is unimportant since $d_p(s)$ does not affect the physical solution.

## 3.6. Representation in Terms of $Q_+$ and $Q_-$

To determine the long-time behavior of $Q_{10}(t)$, we need to know the behavior of $Q_p(s)$ near the origin. Thus, we would like to know the functions $q_+(s)$ and $q_-(s)$ of the representation,

$$Q_p(s) = q_+(s) Q_+(s) + q_-(s) Q_-(s) \tag{38}$$

From Section 3.4, we know that $Q_+$ and $Q_-$ can be represented in terms of $Q_g$ and $Q_d$,

$$Q_\pm(s) = g_\pm(s) Q_g(s) + d_\pm(s) Q_d(s) \tag{39}$$

Together, Eqs. (37)–(39) imply

$$q_-(s)/q_+(s) = -g_+(s)/g_-(s) \tag{40}$$

Thus, the solution for the Laplace transform is

$$\hat{f}(s) = \frac{Q_+(s/\varepsilon) - g_+(s) Q_-(s/\varepsilon)/g_-(s)}{Q_+(s) - g_+(s) Q_-(s)/g_-(s)} \tag{41}$$

The functions $g_+(s)$ and $g_-(s)$ are determined from the asymptotic forms of $Q_+(s)$ and $Q_-(s)$. The tail of the series (30) dominates for $s$ large, so the asymptotic forms can be obtained by solving the large-$n$ form of the recursion relation (33):

$$a_n^\pm \cong a_{n-1}^\pm \varepsilon^{n+\gamma_\pm+1}/v$$

This is solved by $a_n^\pm \cong C_n^\pm$, where

$$C_n^\pm = C_\pm' \, \varepsilon^{n(n+1)/2 + n(\gamma_\pm + 1)}/v^n \tag{42}$$

in which the constants $C'_\pm$ are determined by requiring

$$\lim_{n \to \infty} C_n^\pm / a_n^\pm = 1$$

This gives

$$C'_\pm = \prod_{n=1}^{\infty} \left( 1 - \frac{\varepsilon^{\gamma_\pm + n}}{v} + \frac{e^{2\gamma_\pm + 2n}}{v} \right)^{-1} \tag{43}$$

Insertion of Eqs. (42) and (43) into Eq. (30) and extension of the sum to include the infinitesimal terms with $-\infty < n < 0$ yields the asymptotic forms for $Q_+$ and $Q_-$,

$$Q_\pm \sim C_\pm \hat{q}(\varepsilon^{\gamma_\pm} s) \, s^{-(\ln s/2 \ln \varepsilon) - (3/2) + \ln v/\ln \varepsilon} \tag{44}$$

where $C_\pm \equiv C'_\pm \exp[-\frac{1}{2} \ln^2(\varepsilon^{\gamma_\pm + 3/2}/v)/\ln \varepsilon]$, and the function $\hat{q}(s)$ in Eq. (44) is given by

$$\hat{q}(s) = \sum_{n = -\infty}^{\infty} \exp\{\frac{1}{2}[n + \frac{1}{2} + \ln(s/v)/\ln \varepsilon]^2 \ln \varepsilon\} \tag{45}$$

and is manifestly log periodic. Together, Eqs. (34) and (44) imply

$$g_\pm(s) = C_\pm \hat{q}(\varepsilon^{\gamma_\pm} s) \tag{46}$$

Equations (30), (33), (41), and (46) fully specify the solution $\hat{f}(s)$ in terms of sums over elementary functions.

## 3.7. Large-$t$ Behavior of $R_{10}(t)$

The functions $R_{10}(t)$ is obtained from $f(t)$ by the elementary scale transformation of Section 3.3. In turn, $f(t)$ is obtained by Bromwich inversion of $\hat{f}(s)$. The large-$t$ behavior of $f(t)$ is determined by the behavior of $\hat{f}(s)$ near the singularity with the largest value of Re($s$). From Eq. (37) one can see that $\hat{f}(s)$ has singularities only at the zeros of $Q_d(s)$ and the singularities of $Q_d(s)$ and $Q_d(s/\varepsilon)$. The singularities of $Q_d$ occur only at $s = 0$ and $s = \infty$, as one can see from the representation of Eqs. (34) and (36). Furthermore, because $f(t)$ decays, there exist no zeros of $Q_d(s)$ with Re($s$) $\geqslant 0$. Therefore, the only singularity of $\hat{f}(s)$ affecting the Bromwich inversion is the branch point at $s = 0$.

Near the origin $\hat{f}$ has the form

$$\hat{f}(s) \cong r(s) + h(s) s^{(\gamma_- - \gamma_+)} \tag{47}$$

where $r(s)$ is analytic, and

$$h(s) = (C_+/C_-)(\varepsilon^{-\gamma_+} - \varepsilon^{-\gamma_-}) \, \hat{q}(\varepsilon^{\gamma_+} s)/\hat{q}(\varepsilon^{\gamma_-} s)$$

is log periodic and, so, may be written as a Fourier series,

$$h(s) = \sum_{n=-\infty}^{\infty} \tilde{h}_n \exp(i2\pi n \ln s/\ln \varepsilon) \qquad (48)$$

Calculation of the inverse Laplace transform is facilitated by noting that Eqs. (47) and (48) imply that $\hat{f}(s)$ has the form of an infinite series of fractional powers of $s$,

$$\hat{f}(s) \cong r(s) + \sum_n \tilde{h}_n s^{\beta_n}$$

where

$$\beta_n \equiv \gamma_- - \gamma_+ + i2\pi n/\ln \varepsilon$$

To find $f(t)$, one deforms the Bromwich contour to integrate along the branch cut in the usual way. The result is

$$f(t) \sim -\frac{1}{\pi} t^{-1-\beta_0} \sum \tilde{h}_n \sin(\pi\beta_n) \, \Gamma(1 + \beta_n) \exp(-i2\pi n \ln t/\ln \varepsilon) \quad (49)$$

Thus, for large $t$, $f(t)$ is a function log periodic in $t$ modulated by a power law decay, where the exponent

$$\beta_0 = \gamma_- - \gamma_+ = \left| \frac{\ln(\mu\varepsilon)}{\ln \varepsilon} \right| \qquad (50)$$

The total fraction of particles escaping from state one to state zero is $N_e = \int_0^\infty R_{10}(t) \, dt = \hat{f}(0)/(1 + \mu\varepsilon)$. Using Eqs. (25) and (30) we obtain

$$N_e = \begin{cases} 1, & \mu\varepsilon \leqslant 1 \\ (\mu\varepsilon)^{-1}, & \mu\varepsilon \geqslant 1 \end{cases}$$

The change in behavior when $\mu\varepsilon = 1$ is clarified by considering the ratio of left to right moving particles out of state $i$,

$$p_{i,i-1}/p_{i,i+1} = (\mu\varepsilon)^{-1}$$

When $\mu\varepsilon < 1$, particles move to the left more easily than to the right, and all eventually enter state zero, while when $\mu\varepsilon > 1$, many particles starting in state one never enter state zero.

The moments of $f(t)$ also depend on the behavior of $\hat{f}(s)$ near the origin,

$$\langle t^n \rangle \equiv \frac{\int_0^\infty t^n f(t)\, dt}{\int_0^\infty f(t)\, dt} = \frac{(-d/ds)^n \hat{f}|_{s=0}}{\hat{f}(0)}$$

Since $\hat{f}(t)$ decays as the $(1 + \beta_0)$ power of $t$, only moments with $n < \beta_0$ exist. The moments are readily calculted. For example,

$$\langle t \rangle = -\varepsilon^{1+\gamma+}(1 - \varepsilon)/(\nu - \varepsilon^{1+\gamma+} + \varepsilon^{2+2\gamma+})$$

## 4. DISCUSSION

We have shown that the first passage time distribution, $R_{10}(t)$, in the self-similar Markov chain decays as $t^{-1-\beta_0}$. Other distributions $(R_{mn}, m > n)$ can easily be computed using the convolution condition (15) and the rescaling condition (17). Asymptotically these distributions decay with the same power as $R_{10}$.

The power law decay arises from the infinity of "direct" decay rates with an accumulation point at zero, corresponding to ever more deeply trapped particles. In fact, heuristically one might expect the form

$$R_{10}(t) \simeq \sum_j A^j \exp(-\varepsilon^j t)$$

where the $\varepsilon^j$ represent the direct decay rates. It is easy to see that this form gives a power law decay with an exponent $\ln(A)/\ln(\varepsilon)$, times a log periodic function. Comparision with Eq. (50) gives $A \simeq \varepsilon(\mu\varepsilon)$. Here the factor of $\varepsilon$ arises from coupling to states with larger $j$, and that of $\mu\varepsilon$ from coupling to smaller $j$. This form can in fact be obtained by a perturbation solution of Eq. (12) for $\varepsilon$ small. The log periodic oscillatory modulation arises from the change in rate from $\varepsilon^j$ to $\varepsilon^{j+1}$: the $j$th contribution dominates the $(j + 1)$th for a time period proportional to the inverse of its decay rate.

Other statistical quantities of interest can be obtained directly from the escape rates.[1] For example, the survival probability $P_1(t)$,

$$P_1(t) = \int_t^\infty dt'\, R_{10}(t')$$

decays with an exponent one less than $R$. $P_1(t)$ is related to the recurrence time distribution of Ref. 2. Similarly the correlation function can be obtained through integrals of $P$.

Our analysis has been restricted to the continuous-time Markov chain. For the discrete case, the rescaling property (18) no longer holds, because in addition to the factor $\varepsilon$, there is an unavoidable time scale in the problem, namely, the discretization time. However, for large $j$ the decay time constants will be long compared to the discretization time. Thus, for long-time properties, which are dominated by the large $j$ states, the continuous-time model is appropriate.

To compare our results with the motion near a critical noble torus, the values of $\varepsilon$ and $\mu$ from Eqs. (9) and (10) are used in (50):

$$\varepsilon = g^{-2} \cong 0.381966$$

$$\mu = (g/\xi)^2 \cong 0.139045$$

$$\beta_0 = \left| \frac{\ln(\mu\varepsilon)}{\ln \varepsilon} \right| \cong 3.0500 \tag{51}$$

which gives a decay exponent of 4.05 for $R_{10}$. This could be compared to results obtained by Karney[1] for decay in the quadratic area-preserving map. Unfortunately, for the particular parameter value used in Ref. 1 the rotation number of the outermost critical cricle is $\omega_0 = [0, 5, 1, 13,...]$, and not the golden mean. It is difficult in a numerical experiment to obtain a sufficient orbit length to get beyond the first few levels in the continued fraction; in Fig. 6 of Ref. 1 there appear to be five distinct decay rates, perhaps corresponding to the first five levels of $\omega_0$. Thus, since the $l_m$ for small $m$ are not unity, we cannot expect quantitative agreement between the theory and the experiment.

Of course the succession of decay rates observed in Ref. 1 does qualitatively agree with our analysis, corresponding to the log-periodic modulation in the noble case. An alternative explanation of the various decay rates is the branching to side chains corresponding to other critical curves in the system. Further numerical experiments will be necessary to distinguish between these possibilities.

Chirikov and Shepelyansky[11] have given an alternative decay exponent for the first passage time distribution near the border of stochasticity of the "whisker map." They also use the notion of flux through cantori in their discussion, but assume that the scaling of $\Delta W$ is different than Eq. (7),

$$\Delta W_{j,j+1} = \Delta W_{01} g^{2j/\log \delta} \tag{52}$$

where $\delta \cong 1.62795$ is the critical exponent for parameter scaling.[4] Their argument in favor of this assumption is that the effective parameter $k - k_{cr}$

of a cantorus should scale with the distance from the critical circle, but this is hard to justify. Using Eq. (52) in (9) gives $\varepsilon = g^{2/\ln \delta}$ and hence $\beta_0 \cong 1.4971$. This exponent apparently agrees will with numerical experiments, but we believe that this comparison is hampered by the short time of the computations.

## NOTE ADDED IN PROOF

The solution for the particle number, $\hat{N}_j(s)$, of the general birth and death process can be given in terms of a continued fraction expansion[12] analogous to Eq. (25). Our solution represents the limit of this expansion for the self-similar case.

## ACKNOWLEDGMENTS

## REFERENCES

1. C. F. F. Karney, *Physica* **8D**:360 (1983).
2. B. V. Chirikov, Lecture Notes in Physics No. 179 (Springer, Berlin, 1983), p. 29.
3. J. D. Meiss, J. R. Cary, C. Grebogi, J. D. Crawford, A. N. Kaufman, and H. D. I. Abarbanel, *Physica* **6D**:375 (1983).
4. R. S. MacKay, Ph.D. thesis, Princeton University, 1982 (University Microfilms, Ann Arbor, Michigan).
5. R. S. MacKay, J. D. Meiss, and I. C. Percival, *Phys. Rev. Lett.* **52**:697 (1984); and *Physica* **13D**:55 (1984).
6. G. Schmidt, *Phys. Rev.* **22A**:2849 (1980).
7. D. F. Escande, Stochasticity in Hamiltonian systems: Universal aspects, Institute for Fusion Studies, IFSR #147 (1984), preprint.
8. I. C. Percival, in *Nonlinear Dynamics and the Beam-Beam Interaction—1980*, M. Month and J. C. Herrera, eds., AIP Conference Proceedings No. 57 (AIP, New York, 1980), p. 302; S. Aubry and G. Andre, in *Solitons and Condensed Matter Physics*, A. R. Bishop and T. Schneider, eds., (Springer, Berlin, 1978), p. 264.
9. J. Mather, Non-existence of invariant circles, Princeton preprint (1982).
10. R. S. MacKay, personal communication (1984).
11. B. V. Chirikov and D. L. Shepelyansky, *Physica D* **13**:395 (1984).
12. W. B. Jones and W. J. Thron, *Continued Fractions, Analytic Theory and Applications*, Encyclopedia of Mathematics, V.11 (Addison-Wesley, 1980), ch. 11.